The Journal of Immunology

Diverse Antibody Genetic and Recognition Properties Revealed following HIV-1 Envelope Glycoprotein Immunization

Ganesh E. Phad, Néstor Vázquez Bernat, Yu Feng, Jidnyasa Ingale, Paola Andrea Martinez Murillo, Sijy O'Dell, Yuxing Li, John R. Mascola, Christopher Sundling, Richard T. Wyatt and Gunilla B. Karlsson Hedestam

J Immunol 2015; 194:5903-5914; Prepublished online 11 May 2015;
doi: 10.4049/jimmunol.1500122
http://www.jimmunol.org/content/194/12/5903

The Journal of Immunology is published twice each month by
The American Association of Immunologists, Inc.,
9650 Rockville Pike, Bethesda, MD 20814-3994.

Print ISSN: 0022-1767 Online ISSN: 1550-6606.

Diverse Antibody Genetic and Recognition Properties Revealed following HIV-1 Envelope Glycoprotein Immunization

Ganesh E. Phad,* Néstor Vázquez Bernat,* Yu Feng,† Jidnyasa Ingale,† Paola Andrea Martinez Murillo,* Sijy O'Dell,‡ Yuxing Li,†,§ John R. Mascola,‡ Christopher Sundling,*,¶ Richard T. Wyatt,† and Gunilla B. Karlsson Hedestam*

Isolation of mAbs elicited by vaccination provides opportunities to define the development of effective immunity. Ab responses elicited by current HIV-1 envelope glycoprotein (Env) immunogens display narrow neutralizing activity with limited capacity to block infection by tier 2 viruses. Intense work in the field suggests that improved Env immunogens are forthcoming, and it is therefore important to concurrently develop approaches to investigate the quality of vaccine-elicited responses at a higher level of resolution. In this study, we cloned a representative set of mAbs elicited by a model Env immunogen in rhesus macaques and comprehensively characterized their genetic and functional properties. The mAbs were genetically diverse, even within groups of Abs targeting the same subregion of Env, consistent with a highly polyclonal response. mAbs directed against two subdeterminants of Env, the CD4 binding site and V region 3, could in part account for the neutralizing activity observed in the plasma of the animal from which they were cloned, demonstrating the power of mAb isolation for a detailed understanding of the elicited response. Finally, through comparative analyses of mAb binding and neutralizing capacity of HIV-1 using matched Envs, we demonstrate complex relationships between epitope recognition and accessibility, highlighting the protective quaternary packing of the HIV-1 spike relative to vaccine-induced mAbs. ***The Journal of Immunology*****, 2015, 194: 5903–5914.**

The envelope glycoproteins (Envs) of HIV-1 are large Ags, which despite their effective glycan and conformational shield, expose a number of immunogenic regions to the host immune system. Additional determinants may be exposed by Env immunogens that are imperfect mimics of the functional glycoprotein spike, as are most Env subunit vaccines tested preclinically or clinically to date. Generally, primate Abs elicited by Env immunization display narrow neutralizing profiles with limited capacity to block infection of tier 2 viruses. However, intense work in the field suggests that improved Env immunogens are forthcoming and, in anticipation of improved immune responses, it is important to concurrently develop approaches to interrogate the quality of vaccine-elicited responses at a high level of resolution. Although serum binding and neutralization are measured in most Env immunogenicity studies, information is more limited regarding the diversity of Ab subspecificities elicited by Env immunization and their relative representation in the polyclonal B cell response.

Considerably more information is available from studies of chronically HIV-1–infected individuals, where neutralizing Ab responses elicited in several subjects are characterized in great detail. Several of these studies illustrate the extraordinarily complex evolutionary pathways required to develop broadly neutralizing Abs (bNAbs) during infection (1–5), emphasizing the challenge to elicit neutralizing breadth following vaccination. Efforts to mimic infection by stimulating vaccine-induced B cell responses to mature along defined pathways to promote the development of bNAbs have been proposed. These approaches are referred to as B cell lineage immunogen design (6) or Ab germline/maturation targeting strategies (7) and are undergoing current hypothesis-driven testing.

Although bNAbs capable of neutralizing tier 2 viruses develop in some chronically infected individuals, this process almost invariably takes years to evolve. The development of infrequent broad neutralizing activity is usually preceded by neutralizing Ab responses that are restricted to sensitive tier 1 viruses and autologous tier 2 viruses (8, 9). Ab subspecificities responsible for mediating tier 1 neutralization during chronic HIV-1 replication include "F105-like" CD4 binding site (CD4bs)–directed Abs and V region 3 (V3)–directed Abs, demonstrated more than two decades ago by isolation of infection-induced mAbs (10–12). The interest in cloning mAbs from chronically infected individuals has culminated in the recent isolation of several potent and broadly neutralizing mAbs that serve as templates for vaccine design (13–18). Additionally, a subset of these bNAbs is capable of suppressing already established infection in experimental animal models (19, 20).

*Department of Microbiology, Tumor and Cell Biology, Karolinska Institutet, 171 77 Stockholm, Sweden; †International AIDS Vaccine Initiative, Neutralizing Antibody Center, Department of Immunology and Microbial Science, The Scripps Research Institute, La Jolla, CA 92037; ‡Vaccine Research Center, National Institutes of Health, Bethesda, MD 20892; §Institute for Bioscience and Biotechnology Research, University of Maryland, Rockville, MD 20850; and ¶Immunology Division, Garvan Institute of Medical Research, Darlinghurst, New South Wales 2010, Australia

Received for publication January 16, 2015. Accepted for publication April 15, 2015.

This work was supported by the Swedish Research Council, Karolinska Institutet, National Institutes of Health Grant 1P01AI104722-01A1, the National Institutes of Health Intramural Research Program, and the International AIDS Vaccine Initiative. Funding of the International AIDS Vaccine Initiative is made possible by support from many donors, the full list of which is available at http://www.iavi.org.

The sequences presented in this article have been deposited to GenBank (http://www.ncbi.nlm.nih.gov/genbank/) under accession numbers KP271293–KP271344.

Address correspondence and reprint requests to Gunilla B. Karlsson Hedestam, Department of Microbiology, Tumor and Cell Biology, Karolinska Institutet, Box 280, 171 77 Stockholm, Sweden. E-mail address: Gunilla.Karlsson.Hedestam@ki.se

The online version of this article contains supplemental material.

Abbreviations used in this article: bNAb, broadly neutralizing Ab; CD4bs, CD4 binding site; Env, envelope glycoprotein; F, foldon; HA1, hemagglutinin-1; HC, H chain; LC, L chain; V3, V region 3; VH, IgH V gene.

To date, bNAbs have not been elicited by Env immunization, but several studies demonstrate that Abs capable of neutralizing tier 1 viruses are readily induced in experimental systems (21–27) and, as well, in the VAX003 clinical trial (28). In a direct comparison, weaker and less sustained neutralizing Ab titers were detected in the RV144 trial (29) for reasons that are unclear and under investigation. Ab specificities elicited by Env immunization were not defined at the molecular level until relatively recently. Studies now demonstrate the isolation of CD4bs-directed neutralizing Abs from immunized rhesus macaques (30), V3-specific mAbs from Env-inoculated rabbits (31), and isolation of Env-specific mAbs from human subjects enrolled in either the RV144 trial (32, 33) or the GSK PRO HIV-002 trial (34). However, more comprehensive analyses of the genetic and functional properties of mAbs induced by HIV-1 Env immunization are still lacking, and our current understanding of Env vaccine–elicited B cell responses are therefore largely based on analyses of polyclonal plasma or serum samples. The low resolution of these analyses provides limited molecular information about the composition of the induced B cell or Ab response.

To begin to understand primate immune responses to Env immunization, we recently investigated the contribution of individual Ab H chain (HC) V gene segments in Ag-specific IgG-switched memory B cells from rhesus macaques immunized with soluble HIV-1 Env trimers in adjuvant (35). Using a highly specific flow cytometry–based strategy for single B cell sorting, we demonstrate that the pattern of IgH V gene (VH) segments usage among Env-specific memory B cells (based on VH sequences from >500 single cells) is highly diverse, engaging a broad repertoire of VH gene segments similar to that identified in the expressed total IgG-switched memory B cell population. In our present study, we isolated and characterized the genetic properties of 52 cloned Env-specific mAbs, which mapped to distinct epitope regions of Env. We demonstrated that a subset of the mAbs, comprised of mAbs with specificity against the CD4bs or V3, recapitulated the neutralizing activity in the plasma of the animal from which they were cloned. In some instances, these mAbs neutralized viruses beyond the activity measured in the corresponding plasma sample. We further demonstrated that HIV-1 neutralization depends both on epitope recognition on Env and epitope exposure on the matching virus, providing new and detailed information about the B cell response elicited by Env vaccination.

Materials and Methods

Animals and ethics statement

Two rhesus macaques (*Macaca mulatta*) of Chinese origin, designated F124 and F128, described elsewhere (22), were sampled in the present study. The animals were housed at the American Association for the Accreditation of Laboratory Animal Care–accredited Astrid Fagraeus Laboratory at Karolinska Institutet. Housing and care procedures were in compliance with the guidelines of the Swedish Board of Agriculture. The facility has been assigned an Animal Welfare Assurance number by the Office of Laboratory Animal Welfare at the National Institutes of Health. The Local Ethical Committee on Animal Experiments (Stockholms Norra Djurförsöksetiska Nämnd; ethical permit nos. N85/09 and N32/12) approved all procedures. Before inclusion in the study, all animals were tested and confirmed negative for SIV, simian T cell lymphotropic virus, and simian retrovirus type D.

Immunization and sampling

A detailed description of the immunization experiment was described previously (22). Briefly, all animals were inoculated i.m. five times at monthly intervals with soluble gp140 trimers derived from the HIV-1 YU2 isolate encoding a foldon (F) trimerization motif (hereafter referred to as gp140-F) (36) in an adjuvant formulation consisting of AbISCO-100 (Isconova, now Novavax) and CpG-C ODN2395 (Coley/Pfizer). Peripheral blood samples were collected before and after immunization and PBMCs were isolated by density-gradient centrifugation with Ficoll-Hypaque (GE Healthcare) followed by extensive washing in PBS. The PBMCs were then counted and frozen in 90% heat-inactivated FBS and 10% DMSO (Sigma-Aldrich). The mAbs described in the present study were isolated from IgG^+ memory B cells after the fourth immunization from macaque F124, and following the fifth immunization from macaque F128.

Expression and purification of Env glycoproteins

The soluble YU2-derived gp140-F trimers (36) used as the immunogen were produced by transient transfection into FreeStyle 293F suspension cells (Invitrogen) as previously described (37). The Env ligands used in the binding studies were the following trimeric proteins: gp140-F, gp120-F, gp120-F–ΔV3, gp120-F–ΔV1V2, gp140-F–D368R, and the following monomeric proteins: TriMut, TriMut-368/370, TriMut-368/370/474, and gp140-GCN4 were purified by lentil lectin and gel filtration chromatography. The biotinylated gp140-F probe used for single cell sorting by flow cytometry was purified by lentil lectin affinity chromatography and nickel-chelating chromatography (GE Healthcare, Uppsala, Sweden). All probes carried an AviTag for site-specific biotinylation at the C termini of the proteins, and biotinylation was performed with biotin ligase BirA (Avidity, Denver, CO). All Env proteins were from the YU2 strain except the TriMut proteins, which were from HXBc2. The collagen-foldon protein was received from the laboratory of Prof. Rikard Holmdahl at the Karolinska Institutet, recombinant OVA protein was purchased from Sigma-Aldrich, and recombinant influenza hemagglutinin 1 (HA1) was produced as previously described (38).

HIV-1 Env-specific single cell sorting by flow cytometry

The flow cytometric cell sorting details for Env-specific memory B cell isolation from the frozen PBMC samples from immunized macaques F124 and F128 are described elsewhere (35). In brief, Env-specific memory B cells were defined as $CD3^-$, $CD8^-$, Aqua $Blue^-$, $CD14^-$, $CD20^+$, IgG^+, $CD27^+$, IgM^-, gp140-F^+, and were sorted at single-cell density into 96-well PCR plates containing 20 μl cell lysis buffer (35) using a three-laser FACSAria cell sorter and stored at −80°C prior to RT-PCR. In sorts performed for F124, an additional 10 μg/ml carrier RNA (poly(A); Qiagen, Valencia, CA) was included in the lysis buffer.

Single B cell RT-PCR and mAb cloning

Cell lysates from sorted HIV-1 Env-specific single memory B cells from animals F124 and F128 were used as a source of RNA for reverse transcription, and V(D)J sequences were amplified as described previously (35, 39). Briefly, the 96-well plates, containing single B cell, were thawed at room temperature and reverse transcribed to cDNA by addition of random hexamers, dNTPs and SuperScript III reverse transcriptase (Invitrogen). The V(D)J sequences were amplified separately in 25 μl nested PCR reactions using 3 μl cDNA in the first round PCR and 1.5 μl PCR product in the second round of PCR. The HotStar Taq Plus kit (Qiagen) and 5′ leader sequence–specific and 3′ IgG-specific primers were used. PCR products from the positive wells were purified, sequenced (GATC Biotech), and analyzed. In-frame unique sequences were submitted to GenBank. The productive HC and L chain (LC) sequences were reamplified in 25 μl cloning PCR reactions to add the cloning sites using 2 μl nested PCR product with Phusion Hot Start II high-fidelity PCR enzyme (Thermo Scientific) and 5′ and 3′ custom cloning primers containing restriction sites previously described (39, 40).

Cloning PCR products were evaluated on 1% agarose gel for correct size (~450 bp for HC and ~350 bp for κ or λ LC) and then PCR purified. Cloning of the Ab sequences into expression vectors containing human Igγ1 H, Igκ1 L, or Igλ2 L constant regions (40) were performed with FastDigest restriction enzymes (Thermo Scientific) according to the manufacturer's instructions. The digested PCR products were inserted into linearized, shrimp alkaline phosphatase–treated vectors using T4 DNA ligase (Thermo Scientific). XL10-Gold ultracompetent cells were then transformed by heat shock at 42°C for 45 s according to manufacturer's protocol (Agilent Technologies). Positive colonies were verified for insert by PCR. Bacterial colonies containing plasmids with inserts of the correct size were then expanded followed by plasmid purification (Qiagen) and Sanger sequencing (GATC Biotech).

The Env-specific Ab HC sequences used in the present study are available under GenBank accession nos. KF947536–KF948098. The matching LC sequences described here are available under GenBank accession nos. KP271293–KP271344 (http://www.ncbi.nlm.nih.gov/genbank/).

Expression of cloned mAbs

For Ab expression, 15 μg each HC and LC vector DNA was transfected into FreeStyle 293-F cells, cultured in 30 ml FreeStyle 293 expression medium (Life Technologies) at cell density 1×10^6 cells/ml and ≥90% viability, using 30 μl FreeStyle Max reagent (Invitrogen) according to the manufacturer's protocol. After 4–5 d, cell culture supernatants were tested for total Ab production and binding to different HIV-1 Env ligands by ELISA. Cultures containing functional Env-specific Abs were then harvested and purified 7 d after transfection using protein G–Sepharose columns (GE Healthcare). All purified recombinant mAbs were further analyzed by SDS-PAGE under reducing condition using NuPAGE Novex 4–12% Bis-Tris polyacrylamide gels and NuPAGE reducing agent (Life Technologies) according to the manufacturer's instructions.

Ig gene sequence analysis

Single-cell RT-PCR–generated HC and LC sequences were analyzed by using the currently available database of rhesus macaque germline sequences (30) and the IgBLAST tool (41) to identify their V(D)J germline gene segments. CDR3 sequences of HC and LC were extracted with IMGT/V-QUEST (42).

Analysis of Ab subspecificities

The purified recombinant mAbs were tested for their subspecificities in ELISA binding assays using different Env ligands. MaxiSorp 96-well plates (Nunc) were coated with 2 μg/ml gp140-F, gp120-F, gp140-F–D368R, gp120-F–ΔV3, gp120-F–ΔV1V2, gp140-GCN4, collagen-foldon, OVA, or HA1 in PBS overnight at 4°C. Next, wells were washed six times with wash buffer (PBS with 0.05% Tween 20) and then blocked for 1.5 h at 37°C with blocking buffer (2% w/v nonfat dry milk, Sigma-Aldrich). The purified mAbs were 5-fold serially diluted in blocking buffer, starting with an initial concentration of 10 μg/ml and incubated for 1.5 h at 37°C. The secondary Ab, HRP-conjugated goat anti-rhesus (Nordic-MUbio) or anti-human (Jackson ImmunoResearch Laboratories) IgG Fcγ was added at 1:10,000 dilution in wash buffer followed by 1 h incubation at room temperature. After washing the wells six times with washing buffer, the Ab binding signal was developed for 5 min by adding 3,3′,5,5′-tetramethylbenzidine (Life Technologies). The reaction was stopped by adding an equal volume of 1 M H_2SO_4. The absorbance or OD was measured at 450 nm. Binding curves were fit by nonlinear regression using GraphPad Prism version 6 software.

For mAbs that remained unmapped by these probes, additional differential binding ELISA assays were performed as described previously (43). Briefly, ELISA plates were coated with 2 μg/ml of either TriMut core gp120 or TriMut core 368/370/474 overnight at 4°C. The TriMut core contains the I423M, N425K, and G431E mutations that inhibit CD4 binding, whereas TriMut core 368/370/474 possesses three additional mutations in the CD4bs (D368R, E370F, and D474A) that eliminate binding by all known CD4bs-directed Abs. The glycan-specific bNAb, 2G12 or CD4bs-directed bNAb, VRC01, and the non-bNAb, b6, were used as controls in this assay. After blocking the plates with nonfat milk and FBS, the plates were incubated with 5-fold serial dilutions of the NHP mAbs with an initial starting concentration of 10 μg/ml. After washing, HRP-conjugated anti-human IgG (1:5000) was added for detection. The plates were then developed by adding 3,3′,5,5′-tetramethylbenzidine chromogenic substrate (Life Technologies) and stopped by sulfuric acid. Absorbance was measured at 450 nm.

Fine mapping of the V3-specific mAbs was performed by using twelve 15-mer peptides, overlapping by 11 residues, spanning the V3 of strain YU2 (GenScript). A full-length YU2 V3 peptide was included as a positive control. All peptides were used at the concentration 2 μg/ml to coat the ELISA plates, and the assays were performed as described above, with the exception that the purified V3-directed mAbs were used in 3-fold dilution series in blocking buffer, starting with an initial concentration of 10 μg/ml.

Binding assays for DJ263.8, MW965.26, SS1196.01, and JRFL

To assess the binding of isolated mAbs to monomeric gp120 dissociated from pseudoviruses or Env-transfected 293T cells, a sandwich ELISA was conducted as previously described (44). Briefly, ELISA plates were coated with the sheep polyclonal Ab D7324, which is specific for the gp120 C5 region. Supernatants containing gp120 shed from DJ263 or JRFL Env transiently expressed in transfected cells from plasmid DNA, or, alternatively, pseudovirus lysates of MW965 and SS1196 were added to the ELISA wells and incubated at 37°C for 2 h to accomplish gp120 capture. ELISA reactions were then developed as described above. The pseudovirus lysates were generated by solubilization in 0.5% Triton X-100 at 37°C for 1 h.

HIV-1 neutralization assays

Neutralization assays were performed using a single-round infectious HIV-1 Env pseudovirus assay with TZM-bl target cells (45). To determine the Ab concentration and the serum dilution that resulted in a 50% reduction in relative luciferase units, serial dilutions of the mAbs and the sera were performed and the neutralization dose-response curves were fit by nonlinear regression using a five-parameter hill slope equation using the R statistical software package. Neutralization capacities of mAbs were reported as the Ab concentration resulting in 50% virus neutralization (IC_{50}), whereas the result for sera were reported as the serum neutralization ID_{50}, which is the reciprocal of the serum dilution producing 50% virus neutralization. Diverse HIV-1 virus isolates were used in the neutralization assays. The sources of the Env-encoding plasmids were as follows: ADA, 89.6, and YU2 (Dana Gabuzda, Dana Farber Cancer Institute) SF162 (Leo Stamatatos, Seattle Biomedical Research Institute), and JRFL and JRCSF (James Binley, Torrey Pines Institute). The BaL.26 (46) and SS1196.1 (45) Envs were previously described, and the clade A DJ263.8 sequence was cloned from virus provided by Francine McCutchan and Vicky Polonis (U.S. Military HIV Research Program). The clade C MW965 Env plasmid was obtained from the AIDS Research and Reagent Repository.

Results

Vaccine-elicited mAbs recognize distinct subdeterminants of Env

We used a flow cytometry–based strategy for single cell sorting Ag-specific IgG-switched memory B cells from rhesus macaques immunized with soluble HIV-1 gp140-F trimers (herein referred to as Env) administered in adjuvant (35). Individual Env-specific memory B cells were sorted based on expression of cell-surface CD20, CD27, and IgG, as well as by Ag-specific binding to a fluorochrome-conjugated Env trimer probe as previously described (30). As an example, we show a sorting experiment in which the Env-specific population was found to be 0.14% of the total input cells corresponding to 4% of the IgG^+ memory population (Fig. 1A). Next, HC V(D)J sequences from sorted Env-specific memory B cells were amplified with nested RT-PCR as previously described (39). Following processing to remove unproductive sequences, V(D)J gene segments were assigned using the currently available database of rhesus macaque germline sequences (30) and IgBLAST followed by CDR3 extraction using IMGT/V-QUEST. Of these amplicons, 52 HC VDJ and 52 matching LC VJ sequences from two NHP donors were cloned and expressed as functional mAbs.

The resulting mAbs were evaluated for binding to HIV-1 gp140-F by ELISA and were confirmed to be immunogen and probe specific. We next mapped the subspecificities of the 52 functional mAbs using a set of probes based on the same YU2 HIV-1 strain as the gp140-F trimers used for immunization, all described previously. The probes included the full-length gp140-F glycoprotein, a trimeric form of gp120 (gp120-F) containing a deletion of the gp41 ectodomain sequence from gp140-F and selectively truncated versions of gp120-F with deletions of variable regions 1 and 2 (gp120-F–ΔV1V2) or V region 3 (gp120-F–ΔV3) and, as well, a gp140-F probe carrying the 368D/R mutation (gp140-F–D368R) that can be used to detect Ab reactivity directed to the gp120 CD4bs. All probes were previously described (47, 48). For mAbs that remained unmapped with this set of probes, we included three additional probes, TriMut, TriMut-368/370, and TriMut-368/370/474 (21, 43), which allowed the identification of CD4bs-directed mAbs, which were not sensitive to the D368R mutation alone (Supplemental Fig. 1). We also included a trimeric gp140 protein stabilized with a heterologous trimerization motif from the GCN4 transcription factor (gp140-GCN4) (49), a trimeric collagen probe stabilized by the foldon motif, collagen-F, and two negative control proteins, influenza hemagglutinin and OVA. Collectively, these probes allowed us to map the gp140-F–elicited mAbs to the

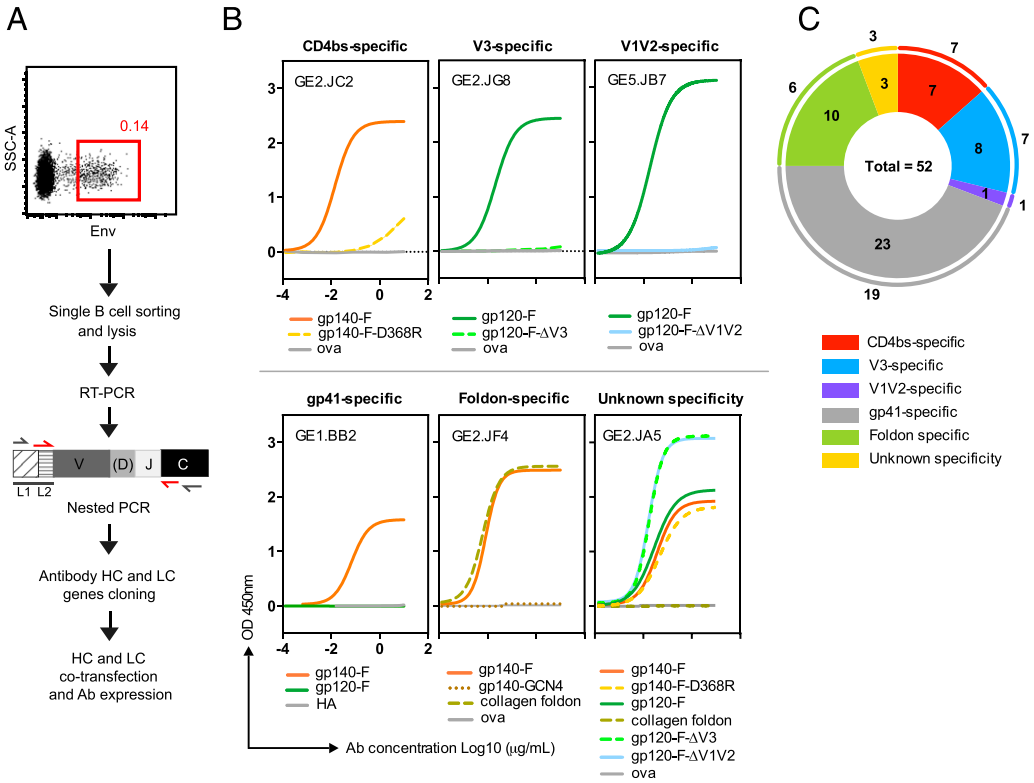

FIGURE 1. Isolation of Env vaccine mAbs and epitope mapping. (**A**) Schematic of Env-specific memory B cell sorting followed by amplification, cloning, and expression of Ab HC and LC. (**B**) Representative ELISA binding curves showing the epitope mapping using YU2 Env ligands as follows: gp140-F and gp140-F–D368R (CD4bs specific), gp120-F and gp120-F ΔV3 (V3 specific), gp120-F and gp120-F–ΔV1V2 (V1V2 specific), gp140-F and gp120-F (gp41 specific), and gp140-F, gp140-GCN4, and collagen foldon (foldon specific). mAbs that could not be mapped with this set of the probes used in this study were defined as unknown specificity. OVA or influenza HA1 were used as controls. Titration curves are shown as $\log_{10}$ dilutions (μg/ml). (**C**) The pie chart demonstrates the distribution of Env-specific mAbs based on their epitope specificity with the total number of mAbs indicated in the center. The color of each slice represents a different Env specificity—red, CD4bs specific; blue, V3 specific; purple, V1V2 specific; gray, gp41specific; green, foldon specific; orange, unknown specificity, and the area of the slice is proportional to the total number of mAbs against a given specificity. The numbers outside each colored slice indicate the number of unique clones for each of the specificities.

following possible subdeterminants of Env: the V1V2 region, V3, gp41, the foldon motif, and the CD4bs. All binding curves from the mapping studies are shown in Supplemental Fig. 1, and representative binding curves are shown in Fig. 1B. A summary of the specificities of the isolated mAbs is shown in Fig. 1C. The numbers inside each "slice" of the pie chart indicate the total number of mAbs against a given specificity, whereas the numbers outside each slice indicate the number of unique clones for each of the specificities. From this analysis we mapped 1 mAb to the V1V2 region, 8 mAbs to V3, 23 mAbs to gp41, 10 mAbs to the foldon motif, 7 mAbs to the CD4bs, and 3 mAbs that could not be mapped with this set of probes.

Env-specific mAbs against distinct epitope regions are genetically diverse

We next examined the genetic properties of the cloned mAbs. We first assigned each Ab HC and LC sequences to the closest germline sequence based on the currently available database for rhesus macaque V(D)J gene segments (30). We then analyzed VH usage and found a marked diversity of gene segment usage among the different Env-specific mAbs, with 21 segments used out of a total 61 VH gene segments in the current rhesus macaque database (Fig. 2A). The bars in Fig. 2 indicate the number of cloned mAbs using a given VH gene segment, and the dots above each bar indicate the epitope specificity of expressed mAbs using a given segment. In the cases where more than one somatic variant was isolated, a larger dot indicates the number of variants identified. The VH gene segments expressed by all Env-specific cells isolated from the two rhesus macaques (F124, n = 194; F128, n = 189) are shown in the *insert* of Fig. 2A (n = 383), illustrating that the distribution of VH gene segments used among the cloned 52 mAbs was similar to that of the total number of HC transcripts sequenced from these animals (35). Most of the Abs expressed in the total B cell memory repertoire used segments from the VH3 and VH4 families, and this was also the case for the mAbs isolated here. The most frequently used gene segment, VH3.63, was used by B cells expressing BCRs of two different Env subspecificities: gp41-directed and foldon-directed mAbs. In our previous study (35), we detect a significant overrepresentation of the VH5 family ($p < 0.01$, χ^2 test) in the Env-specific B cells compared with the total IgG-switched B cells. In that study, VH5.46 is used with significantly increased frequency in the Env-specific memory B cell pool compared with the total IgG memory B cell pool. In this study, we identified two mAbs that used the VH5.46 gene segment, both V3-directed. Additionally, we identified another gene segment belonging to the VH5 family, VH5.7, which was frequently used. VH5.7 was represented by three different Env subspecificities (CD4bs directed, V3 directed, gp41 directed) and by two unmapped mAbs. Otherwise, we found a broad VH gene usage for all Env subspecificities, suggesting no overall bias toward a given gene segment by any of the epitopes. This is consistent with the notion that Ab HCDR3 region, not predominantly encoded by VH, dictates much of the specificity of typical vaccine-induced Abs, as shown

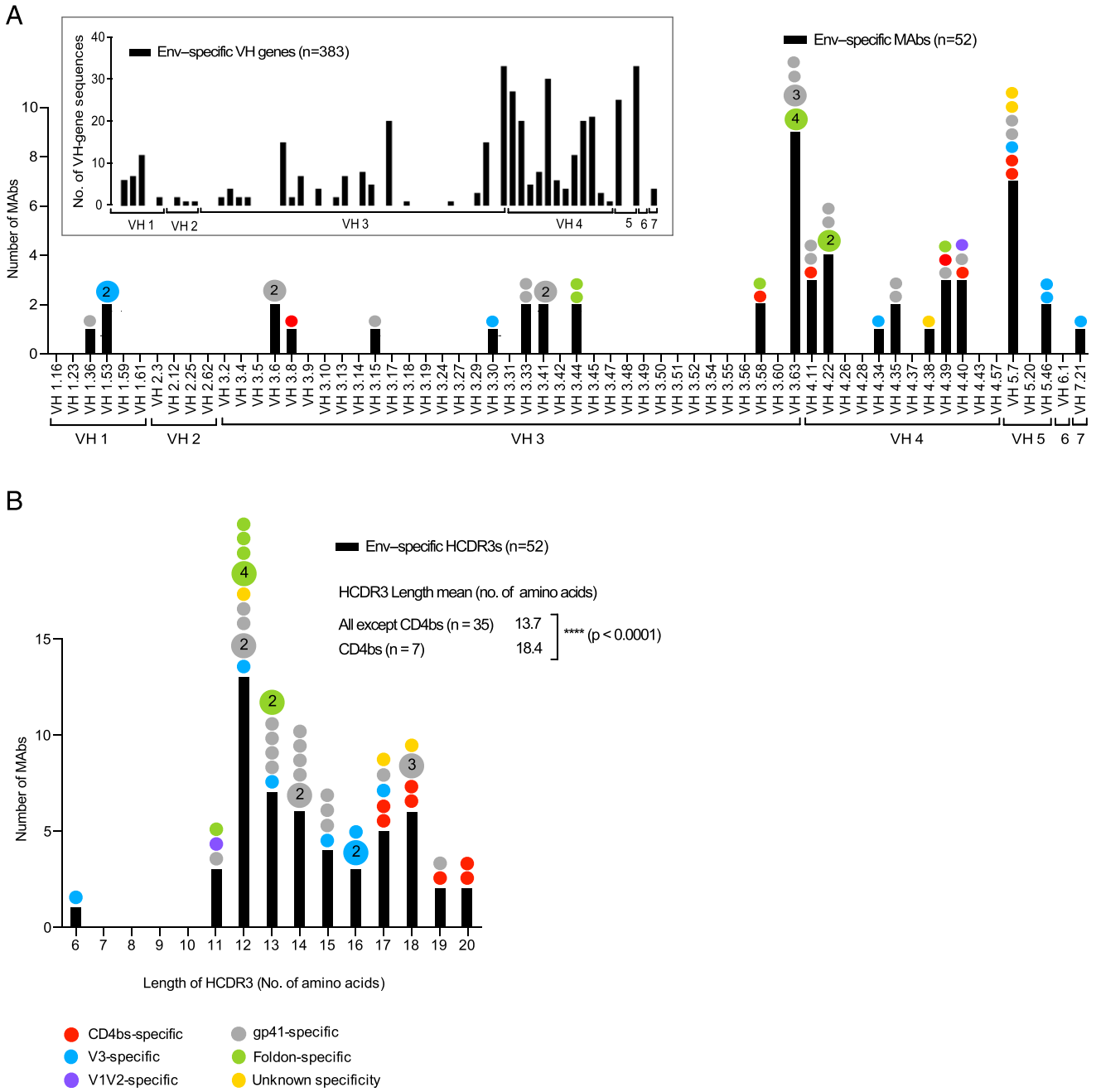

FIGURE 2. Vaccine-induced Env-specific mAbs are genetically diverse. The bars in both (**A**) and (**B**) indicate the number of cloned mAbs (*y*-axis) using a given VH gene segment (A) or HCDR3 length (B). The colored dots above the bars indicate the epitope specificity of expressed mAbs for a given VH gene segment (A) or HCDR3 length (B). Larger dots indicate the number of clonally related mAbs identified. The VH gene segment expression profile by Env-specific IgG^+ memory B cells isolated from the F124 and F128 together (n = 383) is shown in the *inset* in (A).

for previously isolated vaccine-elicited CD4bs-directed mAbs (50, 51).

We also examined the length of the HCDR3 regions of the cloned mAbs and found that they varied between 11 and 20 aa, except for one V3-directed mAb that had a HCDR3 of only 6 aa (Fig. 2B). Interestingly, for the CD4bs-directed mAbs there was a bias toward longer HCDR3 regions, between 17 and 20 aa for the seven mAbs included in the analysis. In contrast, the foldon-specific mAbs studied possessed overall shorter HCDR3s, 11–13 aa. There was no bias toward longer or shorter HCDR3 regions for the other subspecificities for the mAbs examined. The bias toward longer HCDR3s for the CD4bs-directed mAbs compared with the other Ab subspecificities was statistically significant ($p < 0.0001$).

We also analyzed the HCDR3 length of the mAbs together with the larger set of Env-specific (n = 383) and total memory (n = 259) HC sequences obtained from single cell isolation and RT-PCR of VDJ transcripts from animals F124 and F128 described in Sundling et al. (35). This analysis demonstrated that the distribution of HCDR3 lengths plotted for the cloned mAbs was representative also of the larger data set, with most HC sequences encoding HCDR3s of 11–20 aa (Supplemental Fig. 2).

We next examined the LC V gene usage and found that 25 of the mAbs used κ-chains while 27 mAbs used λ-chains. Several different κ and λ V gene segments from VK and VL gene families were used, again consistent with a diverse polyclonal response (Fig. 3, Supplemental Fig. 2). The LC V and J gene usage are

Specificity	Animal	MAb ID	Heavy chain: VDJ gene usage VH	D	JH	HCDR3-IMGT	% SHM nt	% SHM AA	Light chain: VJ gene usage VK	VL	J	LCDR3-IMGT	% SHM nt	% SHM AA
CD4bs-specific MAbs	F124	GE2.JC2	3.58	1	5	TKGRLTFFGLVTNWFDV	3.4	6.3	1.54	-	1	QHYYSTPPT	2.1	4.2
		GE5.JH10	5.7	3	6	AKSRRVTIFGLARDYHGLDS	3.8	6.3	1.19	-	4	LQGYSTPLT	2.5	5.3
		GE2.JA1	5.7	2	2	AKAGCSGINCYLWGTWYFDH	3.7	9.4	-	1.19	2	SAWDSSLSAGL	9.6	13.3
		GE5.JH3	4.40	3	6	ARVANYNFWTGYSNYGLDS	4.1	8.3	-	2.7	1	SSYAAYNTFI	3.7	6.1
	F128	GE2.BD10	4.11	3	5	ARHRGTIFGLVIFNWFDV	7.8	11.5	-	2.7	2	SSYAGSNTGL	1	2.1
		GE2.BB3	4.39	2	5	AMKHCSGFYCYSLAWFDD	5.8	9.4	1.8	-	4	QQYDDLPPT	1	2.1
		GE2.BB9	3.8	2	4	AKGRITVFGLVVTYFDY	3.8	8.3	1.54	-	4	QHYYSNPPT	3.5	7.4
V3-specific MAbs	F124	GE2.JD5 ‡	1.53	2	4	ATGRCSGGVCQPEFEY	5.1	10.4	-	1.18	x1	LSYDSSLSGWV	2.1	6.1
		GE2.JG8 ‡	1.53	2	4	ATGRCSGSVCQPEFDY	3.7	9.4	-	1.18	x1	LSYDSSLSAWV	2.4	5.1
		GE2.JC10	5.46	3	6	AKYYEDDYGQSNYGLDS	5.8	10.4	-	1.19	2	GAWDNSLSTGL	2.7	5.1
		GE2.JF11	5.7	2	4	AKLRCSDSGCYAHFDS	6.5	9.4	-	1.18	x1	LSYDSSLSAWV	2.7	7.1
		GE2.JH1	7.21	6	4	AIIAAAGTPIFDY	8.6	13.5	2.38	-	4	MQALEFPLT	3.3	5.9
		GE5.JC1	4.34	6	4	AREAAD	9.8	13.5	-	2.7	1	SSFAGSNTYI	4.4	6.1
		GE5.JC5	5.46	6	4	AKIAAAYGGFDS	5.8	12.5	-	1.30	x1	QSYDSSLSGWV	3.4	4.1
	F128	GE2.BB5	3.30	3	4	AREQFLDWLSDHFDY	2.3	4.1	-	5.35	x1	CTWHGDSKTWV	2.5	2.9
gp41-specific MAbs	F124	GE2.JE7	3.15	5	4	SQDRIPRGYTFDS	6.6	12.5	-	2.13	1	NSYAGSNTFI	3.4	8.1
		GE2.JC11	3.63	1	1	AKTKYNWNYGLYFDF	3.7	5.2	1.20	-	1	QQHNSYPPT	5.6	10.5
		GE2.JG11	3.33	6	3	ARGSPLIAVAGPKHDAFDF	11.5	14.6	1.27	-	3	QQHNSHPFT	0	0
		GE5.JA2	4.35	6	6	GRQRYSSWSDYGLDS	4.1	7.3	-	1.18	1	LSYDTSLSAYI	3.4	7.1
		GE5.JA3	4.39	4	4	ASARGQWVHLLIDS	3.1	6.3	-	1.30	1	QSYDSSLNTYI	5.1	9.18
		GE5.JB10	4.40	1	4	ARDWLRTYKIDY	2.7	6.3	-	1.27	2	AAWDNSLNGPGL	3.7	4.1
		GE5.JD1	4.22	3	4	ARGIYSGSYYPKFDY	3.7	7.3	-	2.7	1	CSYAGSNTFV	3.7	6.1
		GE5.JD4	4.11	6	4	ARAPRIEATGIFDS	6.8	6.3	-	2.51	1	CSYTISTYI	5.5	7.3
		GE5.JD6	4.35	4	4	ARRQWVRNFDY	4.1	7.3	-	4.36	2	QTWTTGIHGL	4.3	6.1
		GE5.JF2	1.36	4	5	AANTITTRGRFDV	1.7	2.1	-	2.7	x1	SSYAGSNTWV	4.4	7.1
		GE5.JH1	4.11	3	3	ARVLGWGGAFDF	0.7	2.1	1.37	-	2	LQYSSSPYS	4.6	7.4
	F128	GE1.BB2 †	3.41	2	4	ARRMPGTGGLDS	6.5	10.5	1.15	-	3	QQGNSNPPT	2.5	6.4
		GE1.BH6 †	3.41	2	4	ARRMPGTGGLDS	6.5	10.5	1.15	-	3	QQGNSNPPT	6.1	13.8
		GE1.BH7 √	3.6	2	5	ARARVVVSAKWLDV	4.3	6.1	7.5	-	1	LQSKSSWT	3.4	9.2
		GE1.BD2 √	3.6	2	5	SRTRVVVSAKWLDV	4.7	6.1	7.5	-	1	LQSKNSWT	1.7	5.2
		GE1.BB4 •	3.63	2	4	AKDRGSNYYSGSYRYFDY	4.4	8.3	-	1.25	3	EAWDDSLSGVL	1.7	3.1
		GE2.BA7 •	3.63	2	4	AKDRGSNYYSGSYRYFDY	4.4	8.3	-	1.25	3	EAWDDSLSGVL	1.7	3.1
		GE2.BG1 •	3.63	2	4	AKDRGSNYYSGSYRYFDY	4.4	8.3		1.25	3	EAWDDSLSGVL	1.7	3.1
		GE1.BB8	5.7	3	5	AKTYSRIYTWFDV	0.7	2.1	3.30	-	1	QKYRGSPPWP	2.8	5.3
		GE2.BA9	3.63	1	4	AKGRRSAATTFFDY	6.4	11.5	-	4.36	6	QTWTTGSHV	3.3	5.1
		GE2.BE2	3.33	3	4	ARVGGFGLVIRAPNFDY	13.6	19.8	-	2.13	x1	CSYVGSFTWV	2.4	6.1
		GE1.BG3	5.7	3	5	AKSYSRIYTWFDV	1.7	5.2	3.30	-	1	QKYRGSPPWP	3.9	7.4
		GE2.BF3	4.22	2	5	ARRCSGGVCRWFDV	5.1	7.3	1.52	-	3	QHGYGSPFT	9.2	15.8
V1V2	F124	GE5.JB7	4.40	6	3	ARYSGSKGFDF	3.7	6.3	-	3.45	2	YSGDDNNGL	1.1	3.19
Foldon-specific MAbs	F124	GE2.JF4 *	3.63	3	4	AKGGRYENYFDY	4.8	8.3	3.30	-	3	QKYSSSPFT	3.2	3.2
		GE2.JB7 *	3.63	2	4	AKGGSSGNYFDY	5.1	12.5	3.30	-	3	QKYSSSPFT	3.5	5.3
		GE2.JH5 *	3.63	4	4	AKGGDSGNYFYY	3.4	6.3	3.30	-	4	QKYSSPPFT	4.6	8.4
		GE2.JG5 *	3.63	2	4	AKGVFSGNYFDY	6.1	13.5	3.30	-	3	QKYSSLPFT	4	6.3
		GE2.JD10	3.58	4	4	VKGGSRGNYFDY	4.8	6.3	1.9	-	1	QKYDSLPLT	5.4	9.5
		GE5.JB9	4.39	1	4	ARGSYNGNFFVY	8.1	13.5	1.9	-	2	QQYDSLPYS	5.7	10.6
		GE2.JC9	3.44	6	4	VRVAGWYYFDY	1.7	4.2	-	2.7	1	ISYAGSNTFYI	6.4	11.2
	F128	GE2.BB6 #	4.22	1	2	ASSVTGTTRYFDL	4.1	7.3	1.52	-	4	QQAYSNPLT	2.8	4.3
		GE2.BE8 #	4.22	1	2	ATSVTGTTRYFDL	5.8	11.5	1.52	-	4	QQVNSNPYS	3.2	5.3
		GE1.BF10	3.44	7	5	ARAWGGYYGLDS	4.1	9.4	-	8.43	1	ALYMGSGISI	2.4	4.1
Unknown	F124	GE2.JA5	5.7	1	4	AKLGIDGTLSDY	4.1	4.2	-	3.45	2	YSGDDNNGL	2.1	4.3
	F128	GE1.BB3	4.38	4	3	ARIDEHFGYGNYEDALDF	5.1	9.38	1.26	-	4	LQYNSNPLT	2.8	4.3
		GE1.BC3	5.7	3	4	AKSNYNILTGPTNYFDV	1.7	2.08	1.42	-	1	QQDYNIPST	1.8	4.2

Clonal variants are denoted by special characters (‡, †, √, •, *, #)

FIGURE 3. Summary of genetic properties of the vaccine-elicited Env-specific mAbs. V(D)J gene annotations and CDR3 regions of HC and LC of Env-specific mAbs were extracted using IgBLAST and IMGT-VQUEST, respectively. Ab HC and LC sequences with the same V and (*Figure legend continues*)

described in Fig. 3 as well as the HC V, D, and J gene usage and characteristics of the HCDR3 and LCDR3 regions. The length of the LCDR3 region was between 8 and 12 aa, which, as expected, is shorter than the HCDR3 regions due to the lack of a D segment. We also asked whether any of the mAbs were clonally related based on a definition that clonal relatives have the same V(D)J gene usage and the same length and close identity of the HCDR3. We identified only a few clonally related Abs in this set of 52 mAbs as indicated in Fig. 3. Finally, we calculated the degree of somatic hypermutation (SHM) for each Ab at both the nucleotide and amino acid level. We found that the average SHM for the HC V region was 4.9% nt and 8.4% aa and the average SHM for the LC V region was 3.5% nt and 6.2% aa, similar to the level of SHM observed in previous studies of vaccine-elicited Ab responses (30).

Collectively, these data illustrate the genetic diversity and level of SHM of the Env vaccine–elicited Ab response, as well as the diversity among Abs recognizing specific Env epitope regions.

CD4bs- and V3-directed mAbs display distinct HIV-1 neutralization signatures

To examine the neutralizing capacity of the 52 vaccine-induced mAbs analyzed in the present study, we chose a panel of commonly used HIV-1 Env pseudoviruses. The panel included "easy-to-neutralize" viruses represented by tier 1 viruses, including HxBc2, MN, ADA, and SF162 (all clade B), DJ263 (clade A), and MW965 (clade C); viruses that display an intermediate neutralization phenotype, classified as tier 1B viruses, including SS1196, BaL.26, JRCSF, and 89.6 (clade B) and neutralization-resistant tier 2–like viruses, were considered representative of primary circulating strains, such as JRFL and YU2 (clade B) (52).

The vaccine-elicited neutralizing mAbs isolated in the present study were either CD4bs or V3 specific, whereas no neutralizing activity was detected for the gp41-, foldon-, or V1V2-specific mAbs. We therefore focused our subsequent analyses on animal F124, from which four CD4bs-directed mAbs were neutralizing and five of seven V3-directed mAbs were neutralizing. The neutralizing activities of these mAbs are quantified by the IC_{50} values shown in Fig. 4. In brief, we observed distinct neutralization signatures depending on the subspecificity of the Abs. All the CD4bs-directed mAbs neutralized HxBc2, and all but one neutralized the clade A virus, DJ263. These two viruses were not neutralized by any of the V3-directed mAbs. Five viruses in the panel, that is, SF162, SS1196, BaL.26, JRCSF, and MW965, were neutralized by all or most of the V3-directed mAbs, whereas these viruses were not neutralized by the CD4bs-directed mAbs, except in a few isolated cases. Two viruses in this panel, MN and ADA, were neutralized by both the CD4bs- and V3-directed mAbs. One of the CD4bs-directed mAbs, GE5.JH3, displayed superior potency reaching low (<0.05) IC_{50} values against HxBc2, MN, and ADA. GE5.JH3 also neutralized two of the V3-sensitive viruses (SF162 and SS1196) not neutralized by the other CD4bs-directed mAbs, indicating a potentially unique mode of interaction with the viral spike for this mAb.

We also measured the neutralizing activity of the unfractionated plasma from animal F124, shown as ID_{50} values. We included one prebleed sample and one sample collected 1 wk after the fourth immunization, the same time point from which the mAbs were isolated. Six viruses (HxBc2, MN, ADA, SF162, SS1196, and MW965) were neutralized by the post-4 immunization plasma sample, whereas there was no detectable neutralizing activity in the prebleed control sample. These data demonstrate that all neutralizing activity measured in the plasma of F124 could in part be accounted for by the CD4bs- and V3-specific mAbs isolated from the same animal.

The V3-specific mAbs target the crown and flanking N-terminal region

To determine specifically where within V3 the V3-directed mAbs bind, we performed binding studies using the full-length V3 peptide and 15-mer peptides overlapping by 11 residues (Fig. 5A). We included the six V3-specific mAbs from animal F124 (all except GE5.JC1) and one neutralizing V3-specific mAb from animal F128. All seven mAbs bound the full-length peptide, confirming their specificities for V3. Of the 15-mer peptides, only one peptide, peptide 5, was efficiently recognized by the vaccine-elicited mAbs, specifically by GE2.JC10, GE2.JF11, GE2.JG8, GE2.BB5, and GE5.JC5. GE2.JD5 bound peptide 5 only very weakly despite it being a clonal variant of GE2.JG8, suggesting a role for differences in somatic hypermutation between these mAbs (Fig. 5B). These data suggest that a major part of the epitope is contained within the peptide 5 region. To examine the exposure of this epitope region in the context of the three-dimensional architecture of HIV-1 Env, we used the structure of the soluble CD4-complexed JRFL gp120 core containing V3 (53) compared with the core and V3 extracted from the structure of the cleaved, soluble BG505 SOSIP gp140 trimers (54) (Protein Data Bank IDs 2B4C and 4NCO). As shown in Fig. 5C, the peptide 5 region is readily exposed on the post-CD4 JRFL core conformation, whereas V3 is occluded in the BG505 SOSIP structure, which is in the pre-CD4 triggered state. In this native-like conformation, V1, V2, and V3 form a cap at the apex of the trimer, precluding recognition of this V3 epitope in this context and, by inference, on the functional HIV-1 primary isolate spike.

HIV-1 neutralization depends on both epitope recognition and epitope exposure

To further define criteria for Ab neutralization, we focused on three strains, DJ263, MW965, and SS1196, for which we observed a clear difference in the ability of the CD4bs- and V3-directed mAbs to accomplish neutralization. We reasoned that the capacity of an Ab to neutralize depends on both 1) the presence of the cognate epitope on the target Env, assessed by measuring binding capacity, and 2) the exposure of the epitope on the functional virus spike, assessed by measuring neutralizing capacity. To investigate the relative contribution of recognition and exposure, we used supernatants or lysates of cells transfected with the respective Envs to provide nonfunctional, monomeric forms of the gp120 ligands for use in binding studies. We selected three of the V3-specific mAbs and three of the CD4bs-specific mAbs for these analyses.

Starting with the DJ263 virus, we found that all three CD4bs-directed mAbs bound to monomeric DJ263-derived gp120, whereas the V3-specific mAbs exhibited no or very low binding affinity to this gp120 (Fig. 6A, *upper panels*). These results indicate that the inability of the V3-specific mAbs to neutralize DJ263 is due to a lack of the cognate epitope on gp120. Interestingly, inspection of the primary amino acid sequence of DJ263 shows that peptide 5 is conserved in this Env (Supplemental Fig. 3), and thus it is possible that differences outside of the DJ263

J gene, identical CDR3 length, and ≥80% CDR3 identity at the amino acid level were determined as clonal variants and are denoted by special characters: GE2.JD5[‡] and GE2.JG8[‡]; GE1.BB2[†] and GE1.BH6[†]; GE1.BH7[√] and GE1.BD2[√]; GE1.BB4[•], GE2.BA7[•], and GE2.BG1[•]; GE2.JF4*, GE2.JB7*, GE2.JH5*, and GE2.JG5*; and GE2.BB6[#] and GE2.BE8[#].

	F124	Virus											
		Clade B										Clade A	Clade C
		HxBc2	MN	ADA	SF162	SS1196.01	BaL.26	JRCSF	89.6	JRFL	YU2	DJ263.8	MW965.26
Plasma (ID50)	Pre-bleed	<50	<50	<50	<50	<50	<50	<50	<50	<50	<50	<50	<50
	1w post imm.4	908	16660	328	235	3213	116	<50	<50	<50	<50	<50	1378
MAbs (IC50) CD4bs-specific	GE2.JC2	0.138	0.017	0.5	14.6	>40	>40	>40	>40	>40	>40	>40	>40
	GE5.JH10	0.247	1.6	1.4	>40	>40	>40	>40	>40	>40	>40	4.98	>40
	GE2.JA1	0.707	0.125	1.62	>40	>40	>40	>40	>40	>40	>40	9.15	>40
	GE5.JH3	0.048	0.013	0.026	5.86	8	>40	>40	>40	>40	>40	0.313	>40
V3-specific	GE2.JD5*	>40	0.003	0.024	1.85	1.56	1.09	1.28	>40	>40	>40	>40	4.9
	GE2.JG8*	>40	0.005	0.188	2.18	2.42	2.34	11.9	>40	>40	>40	>40	5.67
	GE2.JF11	>40	4.11	0.464	>40	3.22	>40	>40	>40	>40	>40	>40	>40
	GE2.JC10	>40	0.445	0.213	1	0.428	29.7	>40	>40	>40	>40	>40	38.9
	GE5.JC5	>40	4.01	0.202	2.45	0.689	>40	>40	>40	>40	>40	>40	30.2

* Clonal variants

ID50	IC50 (μg/ml)
>5000	<0.10
500-5000	0.10 -1
50-500	1-10
<50	>10-40
	>40

FIGURE 4. HIV-1 neutralizing activity of Env-specific mAbs. The pre- and postimmunization plasma and the CD4bs-directed and V3-specific mAbs isolated from animal F124 were tested for their capacities to neutralize a panel of Env pseudoviruses. The plasma dilution and the mAb concentration inhibiting 50% of viral entry are shown as neutralization ID_{50} and IC_{50} values, respectively. The ID_{50} values are color coded where red indicates (>5000), orange (500–5000), yellow (50–500), and white (<50) whereas the IC_{50} values in red indicates (<0.1 μg/ml), dark orange (0.1–1 μg/ml), light orange (1–10 μg/ml), yellow (10–40 μg/ml), and white (>40 μg/ml).

peptide 5 contribute to recognition by these YU2-derived V3-directed mAbs. In contrast, the CD4bs-directed mAbs bind the monomeric Env and neutralize the functional virus spike, demonstrating that the cognate CD4bs epitope is both present and available for Ab binding on this virus. For MW965, binding of monomeric gp120 and an association to neutralize virus was observed for two of the three V3-specific mAbs, whereas a lack of binding was associated with a similar lack of neutralizing capacity for the CD4bs-directed mAbs (Fig. 6A, *middle panels*). Overall, for the "easy-to-neutralize" tier 1A viruses DJ263 and MW965, the Ab binding profile to monomeric gp120 correlated well with the neutralizing activity.

For SS1196, we detected a different relationship between monomeric binding and virus neutralization. Efficient binding to gp120 by both the V3- and CD4bs-directed mAbs was detected by ELISA, which was associated with virus neutralization by all three V3-specific mAbs, but for only one of the CD4bs-directed mAbs, GE5.JH3 (Fig. 6A, *lower panels*). From these results we interpret that SS1196 gp120 contains the epitope for both the V3- and the CD4bs-directed mAbs, but that V3 is exposed on the SS1196 functional spike whereas the CD4bs is less accessible. This is consistent with its classification as a tier 1B virus, which is more neutralization resistant presumably due to steric hindrance of certain neutralizing Ab epitopes by quaternary spike packing. Furthermore, monomeric JRFL gp120 was also well recognized by both the CD4bs- and V3-directed mAbs, but none of these Abs neutralized the JRFL virus, consistent with the tight packing of tier 2 virus Env spikes and their resistance to current vaccine-elicited V3- and CD4bs-directed mAbs.

To further investigate the question of recognition versus exposure, we generated a variant of SS1196 that lacked the site for N-linked glycosylation at position 301 and we compared the ability of the V3- and CD4bs-directed mAbs to neutralize the parental SS1196 virus compared with the SS1196Δ301 variant. We found that SS1196Δ301 was sensitive to the CD4bs-directed mAbs and displayed greatly increased sensitivity to the V3-directed mAbs. These data illustrate that glycan shielding at this position effectively prevents recognition of the functional spike by CD4bs-directed Abs and partly prevents recognition of V3-directed Abs. We performed a similar comparison of binding versus neutralization using the JRFL strain, which was not neutralized by any of the Env-elicted mAbs (Fig. 4), but for which there already existed an engineered viral variant lacking a site for N-linked glycosylation at position 301 (JRFLΔ301). We previously showed that removal of the 301 glycan rendered JRFL sensitive to several non-bNAb CD4bs-directed mAbs (30, 55), illustrating effective glycan shielding at this position. In this study, we found that all V3- and two of the CD4bs-directed mAbs neutralized the JRFLΔ301 virus (Fig. 6B), suggesting a close relationship between exposure of the CD4bs and V3 on tier 2 viruses. In sum, these studies suggest that the capacity to achieve neutralization depends both on the presence of the cognate epitope on the specific Env gp120 and relative accessibility of a given epitope in the context of the native, functional virus spike.

Discussion

Successful vaccination stimulates polyclonal B cell responses directed against multiple epitopes on target Ags of a given pathogen. The precise specificities of Abs that mediate protection by antiviral vaccines are usually not known, as this level of resolution requires the isolation of mAbs from vaccine recipients, an endeavor that is rarely undertaken if the vaccine is considered to be effective. In contrast, for vaccines that do not induce desired Ab responses, such as the HIV-1 Env immunogens studied to date, mAb isolation provides concrete information about the fine specificities of the response. This analysis both increases our understanding of biological events taking place following vaccination and reveals the fine specificities that are induced by a given immunogen (30, 50,

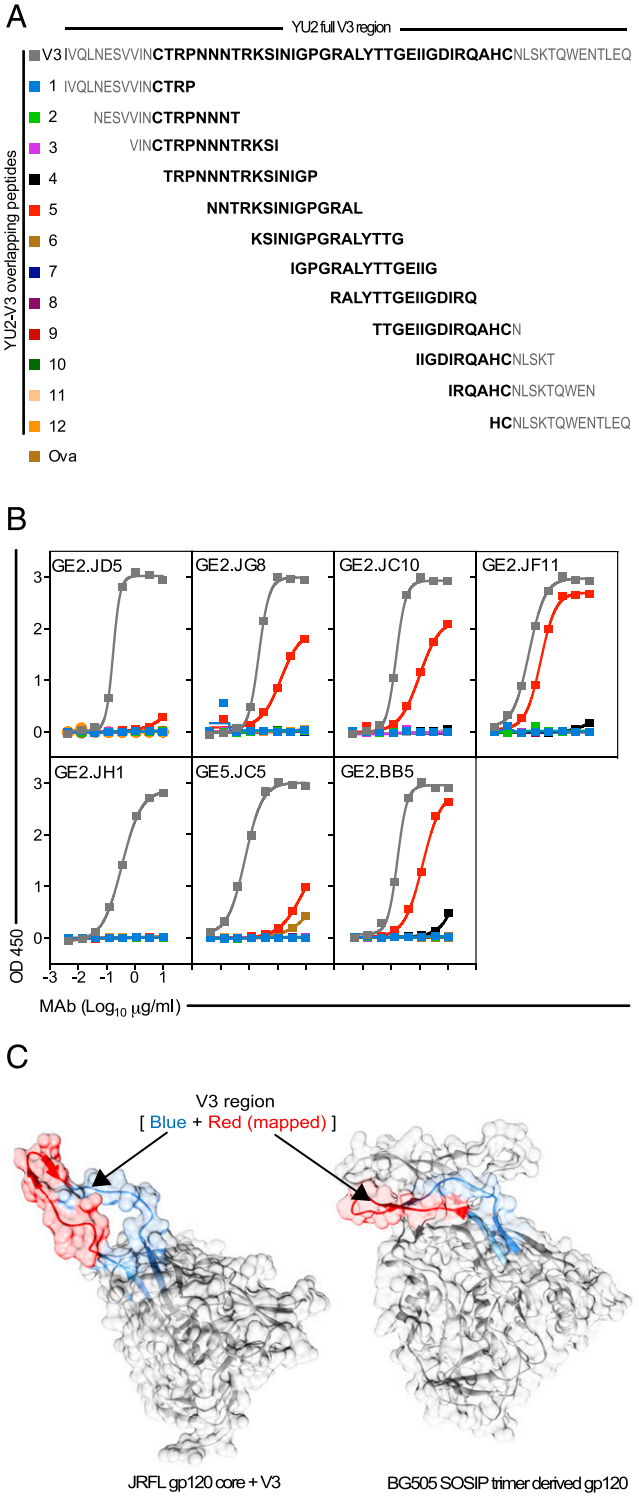

FIGURE 5. Illustration of the epitope region targeted by the vaccine-elicited V3-directed mAbs. (**A**) Amino acid sequences of the full-length YU2 V3 peptide (indicated in bold letters) and twelve 15-mer peptides overlapping by 11, where each peptide is indicated by a number and a color. (**B**) Binding curves of the isolated V3-directed mAbs to the overlapping peptides. (**C**) Surface-rendered crystal structures of two HIV-1 Envs—CD4-complexed JRFL gp120 core (Protein Data Bank ID 2B4C) and the cleaved, soluble BG505.SOSIP gp120 in native state (Protein Data Bank ID 4NCO) (gray)—generated with chimera (65) indicate structural rearrangement of the V3 loop (blue and red) in the post-CD4 binding (JRFL gp120 core) and pre-CD4 triggered (BG505.SOSIP) conformations. The peptide region to which the V3-specific mAbs bind is shown in red and the rest of V3 is shown in blue.

51). This information can guide the design of improved immunogens aimed to favorably alter the elicited B cell response to accelerate the development of HIV-1 vaccine candidates. In the present study, we demonstrate engagement of a broad set of VH genes to multiple specificities, but such analysis is also ongoing for immunogens designed to target specific VH genes, such as the B cell germline engagement immunogen design approach (6).

In the present study, we isolated a set of mAbs elicited by immunization with a model Env trimer immunogen (22). We sorted single Env-specific memory B cells and sequenced their V(D)J transcripts, revealing a highly polyclonal, Env-specific VH repertoire usage. We cloned matching HC and LC pairs resulting in 52 Env-specific mAbs, of which 25% were neutralizing. The neutralizing mAbs, which were either CD4bs or V3 specific, in part recapitulated the neutralizing activity observed in the plasma of the animal from which they were isolated. Interestingly, the CD4bs-directed mAbs neutralized DJ263, a virus that was not detectably neutralized by the plasma. Similarly, two of the V3-directed mAbs neutralized JRCSF, which was not neutralized by the plasma. These results demonstrate that enrichment of distinct specificities through mAb isolation can reveal additional neutralizing activities, providing considerably more information from a given preclinical or clinical vaccine trial. Furthermore, the higher resolution provided by mAb isolation confirms that Env-based vaccines can elicit CD4bs- and V3-directed neutralizing Abs and is consistent with studies using adsorption and competition assays on unfractionated plasma or serum samples (21, 48, 56–58). Among the cloned mAbs, additional Env subspecificities identified were composed of gp41 (n = 23) and the V1V2 region (n = 1). The latter mAb may be worthy of further investigation, because studies of the RV144 clinical trial suggested a correlation between V1V2-directed Abs and vaccine-induced protection (59, 60), stimulating a renewed interest in mAbs against this determinant (33).

The present study reveals that, remarkably, all V3-specific mAbs were directed against a linear determinant on the N-terminal flank of the V3 crown. Consistent with this specificity, this region is expected to be exposed on V3-sensitive tier 1 viruses such as MN, ADA, and SF162. Interestingly, SS1196, classified as a tier 1B virus, was also neutralized by the V3-specific mAbs, but not by most of the CD4bs-directed mAbs, suggesting an intermediate Env conformation between tier 1A and tier 2 viruses. By comparing binding versus neutralization of SS1196 gp120 by selected mAbs, we demonstrated that the CD4bs-directed mAbs recognized their cognate epitope, but they were unable to access it on the functional spike, consistent with epitope masking of conserved regions on more neutralization-resistant viruses. Interestingly, a variant of SS1196 lacking the site for N-linked glycosylation at position 301, SS1196Δ301, was sensitive to the CD4bs-directed mAbs and displayed greatly increased sensitivity to the V3-directed mAbs, illustrating that glycan shielding at this position effectively prevents recognition of the functional spike by CD4bs-directed Abs and partly prevents recognition of V3-directed Abs. Similarly, the inability of the V3-specific mAbs to neutralize tier 2 viruses such as JRFL is likely due to steric hindrance, because removal of the N-linked glycan at position 301 of JRFL to generate the JRFLΔ301 virus rendered this tier 2 virus sensitive to both V3- and CD4bs-directed mAbs. These data are consistent with the structural data of the soluble SOSIP trimers that indicate that these two epitope regions are proximal to one another. In contrast, the lack of HXBc2 neutralization by the V3-specific Abs can be explained by a mismatch of V3s between these Envs, as HxBc2 gp120 possesses an insertion of two residues near its V3 crown (Supplemental Fig. 3). Collectively, these studies show that the

A

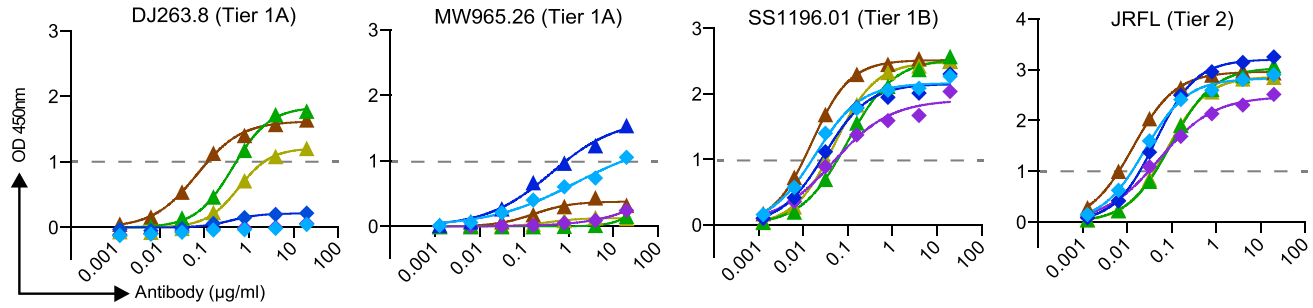

	MAb ID	DJ263.8 Neutralization IC50	DJ263.8 Binding OD (4μg/ml)	MW965.26 Neutralization IC50	MW965.26 Binding OD (4μg/ml)	SS1196.01 Neutralization IC50	SS1196.01 Binding OD (4μg/ml)	JRFL Neutralization IC50	JRFL Binding OD (4μg/ml)
CD4bs	GE5.JH10	4.98	High	>40	No/Low	>40	High	>40	High
CD4bs	GE2.JA1	9.15	High	>40	No/Low	>40	High	>40	High
CD4bs	GE5.JH3	0.313	High	>40	No/Low	8	High	>40	High
V3	GE2.JC10	>40	No/Low	38.9	Medium	0.428	High	>40	High
V3	GE2.JG8	>40	No/Low	5.67	High	2.42	High	>40	High
V3	GE5.JC5	>40	No/Low	30.2	No/Low	0.689	High	>40	High

B

	MAb ID	Neutralization IC50 SS1196.01	SS1196.01Δ301	JRFL	JRFLΔ301
CD4bs	GE5.JH10	>50	0.737	>40	10.5
CD4bs	GE2.JA1	>50	0.655	>40	>40
CD4bs	GE5.JH3	22	0.211	>40	1.4
V3	GE2.JC10	4.16	0.005	>40	21.9
V3	GE2.JG8	6.56	0.052	>40	2.35
V3	GE5.JC5	6.49	0.026	>40	30.5

IC50	OD (4μg/ml)	
<0.01	High	>1
0.1-1	Medium	1-0.5
1-10	No/Low	<0.5
>10-40		
>40		

FIGURE 6. Comparison of mAb binding and neutralizing properties. (**A**) *Upper panels*: ELISA binding curves of the vaccine-induced CD4bs- and V3-directed mAbs to monomeric gp120 from DJ263.8, MW965.26, SS1196.01, and JRFL are shown. *Lower panels*: Summary of gp120 binding activity and virus neutralizing activity for DJ263.8, MW965.26, SS1196.01, and JRFL are shown. Binding activity is indicated as OD values at Ab concentration (4 μg/ml) where red indicates high (OD > 1), light orange indicates medium (OD = 1–0.5), and white indicates no/low (OD < 0.5) binding. Virus neutralizing activity is indicated as IC_{50} values and is color coded as described in Fig. 4. (**B**) Comparison of neutralizing activity for SS1196.01 and SS1196.01Δ301 and for JRFL and JRFLΔ301.

availability of mAbs targeting different epitopes on Env and their use in functional assays can greatly facilitate our understanding of HIV-1 neutralizing determinants and relative exposure/accessibility.

Studies of infection-induced V3 mAbs in humans show an overrepresentation of Abs using the human VH5-51 gene segment (61). Human VH5-51–using mAbs are nonbroadly neutralizing and recognize their epitope on V3 in a manner referred to as the "cradle mode" (62). The cradle mode contrasts with the "ladle mode" used by the relatively broadly neutralizing, V3-directed mAb, 447-52D (63). The ortholog of the human VH5-51 gene segment in rhesus macaques is VH5.7, used by one of our V3-specific mAbs, GE2.JF11. Studies of V3-directed mAbs elicited in Env-immunized rabbits resulted in the isolation of the R56 mAb, which binds by the cradle mode via an epitope that overlaps with peptide 5 identified as the target epitope in our present study (31, 64). R56 was shown to neutralize a similar set of viruses as the V3-specific rhesus mAbs isolated in the present study, suggesting that the V3-specific mAbs identified in our study bind by a similar mode of recognition. In contrast, PGT128, a human bNAb isolated from a chronically infected individual, binds farther toward the C-terminal part of V3 to an epitope that also includes the basal N-linked glycans (16).

The CD4bs-specific mAbs isolated in this study display similar neutralizing properties to previously described vaccine-elicited CD4bs-specific mAbs, GE136, GE148, and GE356 (30, 50). Based on mutagenesis and binding studies to define the Ab/Ab interface combined with modeling studies, these mAbs attempt to bind the Env spike by a vertical angle of approach that is not permitted on tier 2 viruses, thus limiting their neutralization capacities to tier 1 viruses only (50, 51). A similar mode of binding is likely for the CD4bs-directed mAbs isolated in the

present study. Similarly to GE136, GE148, and GE356, the CD4bs-directed mAbs described in the present study possess long HCDR3 regions compared with the mAbs recognizing other epitope regions, suggesting that this property is required for access to the CD4bs. Interestingly, one of the CD4bs-directed mAbs, GE5.JH3, was more potent and displayed a modest increase in breadth of neutralization compared with the other vaccine-induced CD4bs-specific mAbs, suggesting a different mode of interaction with the functional spike. Whether Ab specificities displaying broader neutralizing activities exist at some low frequency in these animals is unknown but can be addressed with more selective strategies for B cell sorting.

In sum, the vaccine-induced mAbs described in this study reveal new information about how the primate B cell repertoire responds to Env immunization and demonstrate the utility of mAb isolation for defining the neutralizing Ab activity induced by vaccination. The availability of mAbs against defined epitope regions of HIV-1 Env provides broad utility to probe the antigenic and immunogenic surfaces of existing and forthcoming subunit Env-based vaccine candidates.

Acknowledgments

We thank Dr. Martin Corcoran for critically reading the manuscript.

Disclosures

The authors have no financial conflicts of interest.

References

1. Wibmer, C. K., J. N. Bhiman, E. S. Gray, N. Tumba, S. S. Abdool Karim, C. Williamson, L. Morris, and P. L. Moore. 2013. Viral escape from HIV-1 neutralizing antibodies drives increased plasma neutralization breadth through sequential recognition of multiple epitopes and immunotypes. *PLoS Pathog.* 9: e1003738.
2. Moore, P. L., E. S. Gray, C. K. Wibmer, J. N. Bhiman, M. Nonyane, D. J. Sheward, T. Hermanus, S. Bajimaya, N. L. Tumba, M. R. Abrahams, et al. 2012. Evolution of an HIV glycan-dependent broadly neutralizing antibody epitope through immune escape. *Nat. Med.* 18: 1688–1692.
3. Liao, H. X., R. Lynch, T. Zhou, F. Gao, S. M. Alam, S. D. Boyd, A. Z. Fire, K. M. Roskin, C. A. Schramm, Z. Zhang, et al; NISC Comparative Sequencing Program. 2013. Co-evolution of a broadly neutralizing HIV-1 antibody and founder virus. *Nature* 496: 469–476.
4. Doria-Rose, N. A., C. A. Schramm, J. Gorman, P. L. Moore, J. N. Bhiman, B. J. DeKosky, M. J. Ernandes, I. S. Georgiev, H. J. Kim, M. Pancera, et al; NISC Comparative Sequencing Program. 2014. Developmental pathway for potent V1V2-directed HIV-neutralizing antibodies. *Nature* 509: 55–62.
5. Gao, F., M. Bonsignori, H. X. Liao, A. Kumar, S. M. Xia, X. Lu, F. Cai, K. K. Hwang, H. Song, T. Zhou, et al. 2014. Cooperation of B cell lineages in induction of HIV-1-broadly neutralizing antibodies. *Cell* 158: 481–491.
6. Haynes, B. F., G. Kelsoe, S. C. Harrison, and T. B. Kepler. 2012. B-cell-lineage immunogen design in vaccine development with HIV-1 as a case study. *Nat. Biotechnol.* 30: 423–433.
7. Jardine, J., J. P. Julien, S. Menis, T. Ota, O. Kalyuzhniy, A. McGuire, D. Sok, P. S. Huang, S. MacPherson, M. Jones, et al. 2013. Rational HIV immunogen design to target specific germline B cell receptors. *Science* 340: 711–716.
8. Davis, K. L., E. S. Gray, P. L. Moore, J. M. Decker, A. Salomon, D. C. Montefiori, B. S. Graham, M. C. Keefer, A. Pinter, L. Morris, et al. 2009. High titer HIV-1 V3-specific antibodies with broad reactivity but low neutralizing potency in acute infection and following vaccination. *Virology* 387: 414–426.
9. Gray, E. S., M. C. Madiga, T. Hermanus, P. L. Moore, C. K. Wibmer, N. L. Tumba, L. Werner, K. Mlisana, S. Sibeko, C. Williamson, et al; CAPRISA002 Study Team. 2011. The neutralization breadth of HIV-1 develops incrementally over four years and is associated with $CD4^+$ T cell decline and high viral load during acute infection. *J. Virol.* 85: 4828–4840.
10. Ho, D. D., J. A. McKeating, X. L. Li, T. Moudgil, E. S. Daar, N. C. Sun, and J. E. Robinson. 1991. Conformational epitope on gp120 important in CD4 binding and human immunodeficiency virus type 1 neutralization identified by a human monoclonal antibody. *J. Virol.* 65: 489–493.
11. Matsushita, S., M. Robert-Guroff, J. Rusche, A. Koito, T. Hattori, H. Hoshino, K. Javaherian, K. Takatsuki, and S. Putney. 1988. Characterization of a human immunodeficiency virus neutralizing monoclonal antibody and mapping of the neutralizing epitope. *J. Virol.* 62: 2107–2114.
12. Posner, M. R., T. Hideshima, T. Cannon, M. Mukherjee, K. H. Mayer, and R. A. Byrn. 1991. An IgG human monoclonal antibody that reacts with HIV-1/GP120, inhibits virus binding to cells, and neutralizes infection. *J. Immunol.* 146: 4325–4332.
13. Huang, J., B. H. Kang, M. Pancera, J. H. Lee, T. Tong, Y. Feng, H. Imamichi, I. S. Georgiev, G. Y. Chuang, A. Druz, et al. 2014. Broad and potent HIV-1 neutralization by a human antibody that binds the gp41-gp120 interface. *Nature* 515: 138–142.
14. Huang, J., G. Ofek, L. Laub, M. K. Louder, N. A. Doria-Rose, N. S. Longo, H. Imamichi, R. T. Bailer, B. Chakrabarti, S. K. Sharma, et al. 2012. Broad and potent neutralization of HIV-1 by a gp41-specific human antibody. *Nature* 491: 406–412.
15. Scheid, J. F., H. Mouquet, B. Ueberheide, R. Diskin, F. Klein, T. Y. Oliveira, J. Pietzsch, D. Fenyo, A. Abadir, K. Velinzon, et al. 2011. Sequence and structural convergence of broad and potent HIV antibodies that mimic CD4 binding. *Science* 333: 1633–1637.
16. Walker, L. M., M. Huber, K. J. Doores, E. Falkowska, R. Pejchal, J. P. Julien, S. K. Wang, A. Ramos, P. Y. Chan-Hui, M. Moyle, et al; Protocol G Principal Investigators. 2011. Broad neutralization coverage of HIV by multiple highly potent antibodies. *Nature* 477: 466–470.
17. Walker, L. M., S. K. Phogat, P. Y. Chan-Hui, D. Wagner, P. Phung, J. L. Goss, T. Wrin, M. D. Simek, S. Fling, J. L. Mitcham, et al; Protocol G Principal Investigators. 2009. Broad and potent neutralizing antibodies from an African donor reveal a new HIV-1 vaccine target. *Science* 326: 285–289.
18. Wu, X., Z. Y. Yang, Y. Li, C. M. Hogerkorp, W. R. Schief, M. S. Seaman, T. Zhou, S. D. Schmidt, L. Wu, L. Xu, et al. 2010. Rational design of envelope identifies broadly neutralizing human monoclonal antibodies to HIV-1. *Science* 329: 856–861.
19. Barouch, D. H., J. B. Whitney, B. Moldt, F. Klein, T. Y. Oliveira, J. Liu, K. E. Stephenson, H. W. Chang, K. Shekhar, S. Gupta, et al. 2013. Therapeutic efficacy of potent neutralizing HIV-1-specific monoclonal antibodies in SHIV-infected rhesus monkeys. *Nature* 503: 244–248.
20. Shingai, M., Y. Nishimura, F. Klein, H. Mouquet, O. K. Donau, R. Plishka, A. Buckler-White, M. Seaman, M. Piatak, Jr., J. D. Lifson, et al. 2013. Antibody-mediated immunotherapy of macaques chronically infected with SHIV suppresses viraemia. *Nature* 503: 277–280.
21. Chakrabarti, B., Y. Feng, S. K. Kumar, K. McKee, G. B. Karlsson Hedestam, C. C. Labranche, D. C. Montefiori, J. R. Mascola, and R. T. Wyatt. 2013. Robust neutralizing antibodies elicited by HIV-1 JRFL envelope glycoprotein trimers in nonhuman primates. *J. Virol.* 87: 13239–13251.
22. Sundling, C., M. N. Forsell, S. O'Dell, Y. Feng, B. Chakrabarti, S. S. Rao, K. Loré, J. R. Mascola, R. T. Wyatt, I. Douagi, and G. B. Karlsson Hedestam. 2010. Soluble HIV-1 Env trimers in adjuvant elicit potent and diverse functional B cell responses in primates. *J. Exp. Med.* 207: 2003–2017.
23. Kovacs, J. M., J. P. Nkolola, H. Peng, A. Cheung, J. Perry, C. A. Miller, M. S. Seaman, D. H. Barouch, and B. Chen. 2012. HIV-1 envelope trimer elicits more potent neutralizing antibody responses than monomeric gp120. *Proc. Natl. Acad. Sci. USA* 109: 12111–12116.
24. Sellhorn, G., Z. Kraft, Z. Caldwell, K. Ellingson, C. Mineart, M. S. Seaman, D. C. Montefiori, E. Lagerquist, and L. Stamatatos. 2012. Engineering, expression, purification, and characterization of stable clade A/B recombinant soluble heterotrimeric gp140 proteins. *J. Virol.* 86: 128–142.
25. Malherbe, D. C., N. A. Doria-Rose, L. Misher, T. Beckett, W. B. Puryear, J. T. Schuman, Z. Kraft, J. O'Malley, M. Mori, I. Srivastava, et al. 2011. Sequential immunization with a subtype B HIV-1 envelope quasispecies partially mimics the in vivo development of neutralizing antibodies. *J. Virol.* 85: 5262–5274.
26. Bontjer, I., M. Melchers, T. Tong, T. van Montfort, D. Eggink, D. Montefiori, W. C. Olson, J. P. Moore, J. M. Binley, B. Berkhout, and R. W. Sanders. 2013. Comparative immunogenicity of evolved V1V2-deleted HIV-1 envelope glycoprotein trimers. *PLoS ONE* 8: e67484.
27. Moody, M. A., S. Santra, N. A. Vandergrift, L. L. Sutherland, T. C. Gurley, M. S. Drinker, A. A. Allen, S. M. Xia, R. R. Meyerhoff, R. Parks, et al. 2014. Toll-like receptor 7/8 (TLR7/8) and TLR9 agonists cooperate to enhance HIV-1 envelope antibody responses in rhesus macaques. *J. Virol.* 88: 3329–3339.
28. Berman, P. W., W. Huang, L. Riddle, A. M. Gray, T. Wrin, J. Vennari, A. Johnson, M. Klaussen, H. Prashad, C. Köhne, et al. 1999. Development of bivalent (B/E) vaccines able to neutralize CCR5-dependent viruses from the United States and Thailand. *Virology* 265: 1–9.
29. Montefiori, D. C., C. Karnasuta, Y. Huang, H. Ahmed, P. Gilbert, M. S. de Souza, R. McLinden, S. Tovanabutra, A. Laurence-Chenine, E. Sanders-Buell, et al. 2012. Magnitude and breadth of the neutralizing antibody response in the RV144 and Vax003 HIV-1 vaccine efficacy trials. *J. Infect. Dis.* 206: 431–441.
30. Sundling, C., Y. Li, N. Huynh, C. Poulsen, R. Wilson, S. O'Dell, Y. Feng, J. R. Mascola, R. T. Wyatt, and G. B. Karlsson Hedestam. 2012. High-resolution definition of vaccine-elicited B cell responses against the HIV primary receptor binding site. *Sci. Transl. Med.* 4: 142ra196.
31. Chen, Y., M. Vaine, A. Wallace, D. Han, S. Wan, M. S. Seaman, D. Montefiori, S. Wang, and S. Lu. 2013. A novel rabbit monoclonal antibody platform to dissect the diverse repertoire of antibody epitopes for HIV-1 Env immunogen design. *J. Virol.* 87: 10232–10243.
32. Bonsignori, M., J. Pollara, M. A. Moody, M. D. Alpert, X. Chen, K. K. Hwang, P. B. Gilbert, Y. Huang, T. C. Gurley, D. M. Kozink, et al. 2012. Antibody-dependent cellular cytotoxicity-mediating antibodies from an HIV-1 vaccine efficacy trial target multiple epitopes and preferentially use the VH1 gene family. *J. Virol.* 86: 11521–11532.
33. Liao, H. X., M. Bonsignori, S. M. Alam, J. S. McLellan, G. D. Tomaras, M. A. Moody, D. M. Kozink, K. K. Hwang, X. Chen, C. Y. Tsao, et al. 2013. Vaccine induction of antibodies against a structurally heterogeneous site of immune pressure within HIV-1 envelope protein variable regions 1 and 2. *Immunity* 38: 176–186.

34. Moody, M. A., N. L. Yates, J. D. Amos, M. S. Drinker, J. A. Eudailey, T. C. Gurley, D. J. Marshall, J. F. Whitesides, X. Chen, A. Foulger, et al. 2012. HIV-1 gp120 vaccine induces affinity maturation in both new and persistent antibody clonal lineages. *J. Virol.* 86: 7496–7507.
35. Sundling, C., Z. Zhang, G. E. Phad, Z. Sheng, Y. Wang, J. R. Mascola, Y. Li, R. T. Wyatt, L. Shapiro, and G. B. Karlsson Hedestam. 2014. Single-cell and deep sequencing of IgG-switched macaque B cells reveal a diverse Ig repertoire following immunization. *J. Immunol.* 192: 3637–3644.
36. Yang, X., J. Lee, E. M. Mahony, P. D. Kwong, R. Wyatt, and J. Sodroski. 2002. Highly stable trimers formed by human immunodeficiency virus type 1 envelope glycoproteins fused with the trimeric motif of T4 bacteriophage fibritin. *J. Virol.* 76: 4634–4642.
37. Forsell, M. N., B. Dey, A. Mörner, K. Svehla, S. O'dell, C. M. Högerkorp, G. Voss, R. Thorstensson, G. M. Shaw, J. R. Mascola, et al. 2008. B cell recognition of the conserved HIV-1 co-receptor binding site is altered by endogenous primate CD4. *PLoS Pathog.* 4: e1000171.
38. Sundling, C., P. Martinez, M. Soldemo, M. Spångberg, K. L. Bengtsson, L. Stertman, M. N. Forsell, and G. B. Karlsson Hedestam. 2013. Immunization of macaques with soluble HIV type 1 and influenza virus envelope glycoproteins results in a similarly rapid contraction of peripheral B-cell responses after boosting. *J. Infect. Dis.* 207: 426–431.
39. Sundling, C., G. Phad, I. Douagi, M. Navis, and G. B. Karlsson Hedestam. 2012. Isolation of antibody V(D)J sequences from single cell sorted rhesus macaque B cells. *J. Immunol. Methods* 386: 85–93.
40. Tiller, T., E. Meffre, S. Yurasov, M. Tsuiji, M. C. Nussenzweig, and H. Wardemann. 2008. Efficient generation of monoclonal antibodies from single human B cells by single cell RT-PCR and expression vector cloning. *J. Immunol. Methods* 329: 112–124.
41. Ye, J., N. Ma, T. L. Madden, and J. M. Ostell. 2013. IgBLAST: an immunoglobulin variable domain sequence analysis tool. *Nucleic Acids Res.* 41: W34–40.
42. Brochet, X., M. P. Lefranc, and V. Giudicelli. 2008. IMGT/V-QUEST: the highly customized and integrated system for IG and TR standardized V-J and V-D-J sequence analysis. *Nucleic Acids Res.* 36: W503–508.
43. Feng, Y., K. McKee, K. Tran, S. O'Dell, S. D. Schmidt, A. Phogat, M. N. Forsell, G. B. Karlsson Hedestam, J. R. Mascola, and R. T. Wyatt. 2012. Biochemically defined HIV-1 envelope glycoprotein variant immunogens display differential binding and neutralizing specificities to the CD4-binding site. *J. Biol. Chem.* 287: 5673–5686.
44. Li, Y., S. O'Dell, L. M. Walker, X. Wu, J. Guenaga, Y. Feng, S. D. Schmidt, K. McKee, M. K. Louder, J. E. Ledgerwood, et al. 2011. Mechanism of neutralization by the broadly neutralizing HIV-1 monoclonal antibody VRC01. *J. Virol.* 85: 8954–8967.
45. Li, M., F. Gao, J. R. Mascola, L. Stamatatos, V. R. Polonis, M. Koutsoukos, G. Voss, P. Goepfert, P. Gilbert, K. M. Greene, et al. 2005. Human immunodeficiency virus type 1 *env* clones from acute and early subtype B infections for standardized assessments of vaccine-elicited neutralizing antibodies. *J. Virol.* 79: 10108–10125.
46. Shu, Y., S. Winfrey, Z. Y. Yang, L. Xu, S. S. Rao, I. Srivastava, S. W. Barnett, G. J. Nabel, and J. R. Mascola. 2007. Efficient protein boosting after plasmid DNA or recombinant adenovirus immunization with HIV-1 vaccine constructs. *Vaccine* 25: 1398–1408.
47. Dosenovic, P., B. Chakrabarti, M. Soldemo, I. Douagi, M. N. Forsell, Y. Li, A. Phogat, S. Paulie, J. Hoxie, R. T. Wyatt, and G. B. Karlsson Hedestam. 2009. Selective expansion of HIV-1 envelope glycoprotein-specific B cell subsets recognizing distinct structural elements following immunization. *J. Immunol.* 183: 3373–3382.
48. Douagi, I., M. N. Forsell, C. Sundling, S. O'Dell, Y. Feng, P. Dosenovic, Y. Li, R. Seder, K. Loré, J. R. Mascola, et al. 2010. Influence of novel CD4 binding-defective HIV-1 envelope glycoprotein immunogens on neutralizing antibody and T-cell responses in nonhuman primates. *J. Virol.* 84: 1683–1695.
49. Yang, X., L. Florin, M. Farzan, P. Kolchinsky, P. D. Kwong, J. Sodroski, and R. Wyatt. 2000. Modifications that stabilize human immunodeficiency virus envelope glycoprotein trimers in solution. *J. Virol.* 74: 4746–4754.
50. Navis, M., K. Tran, S. Bale, G. E. Phad, J. Guenaga, R. Wilson, M. Soldemo, K. McKee, C. Sundling, J. Mascola, et al. 2014. HIV-1 receptor binding site-directed antibodies using a VH1-2 gene segment orthologue are activated by Env trimer immunization. *PLoS Pathog.* 10: e1004337.
51. Tran, K., C. Poulsen, J. Guenaga, N. de Val, R. Wilson, C. Sundling, Y. Li, R. L. Stanfield, I. A. Wilson, A. B. Ward, et al. 2014. Vaccine-elicited primate antibodies use a distinct approach to the HIV-1 primary receptor binding site informing vaccine redesign. *Proc. Natl. Acad. Sci. USA* 111: E738–E747.
52. Seaman, M. S., H. Janes, N. Hawkins, L. E. Grandpre, C. Devoy, A. Giri, R. T. Coffey, L. Harris, B. Wood, M. G. Daniels, et al. 2010. Tiered categorization of a diverse panel of HIV-1 Env pseudoviruses for assessment of neutralizing antibodies. *J. Virol.* 84: 1439–1452.
53. Huang, C. C., M. Tang, M. Y. Zhang, S. Majeed, E. Montabana, R. L. Stanfield, D. S. Dimitrov, B. Korber, J. Sodroski, I. A. Wilson, et al. 2005. Structure of a V3-containing HIV-1 gp120 core. *Science* 310: 1025–1028.
54. Julien, J. P., A. Cupo, D. Sok, R. L. Stanfield, D. Lyumkis, M. C. Deller, P. J. Klasse, D. R. Burton, R. W. Sanders, J. P. Moore, et al. 2013. Crystal structure of a soluble cleaved HIV-1 envelope trimer. *Science* 342: 1477–1483.
55. Koch, M., M. Pancera, P. D. Kwong, P. Kolchinsky, C. Grundner, L. Wang, W. A. Hendrickson, J. Sodroski, and R. Wyatt. 2003. Structure-based, targeted deglycosylation of HIV-1 gp120 and effects on neutralization sensitivity and antibody recognition. *Virology* 313: 387–400.
56. Ingale, J., K. Tran, L. Kong, B. Dey, K. McKee, W. Schief, P. D. Kwong, J. R. Mascola, and R. T. Wyatt. 2014. Hyperglycosylated stable core immunogens designed to present the CD4 binding site are preferentially recognized by broadly neutralizing antibodies. *J. Virol.* 88: 14002–14016.
57. Li, Y., S. A. Migueles, B. Welcher, K. Svehla, A. Phogat, M. K. Louder, X. Wu, G. M. Shaw, M. Connors, R. T. Wyatt, and J. R. Mascola. 2007. Broad HIV-1 neutralization mediated by CD4-binding site antibodies. *Nat. Med.* 13: 1032–1034.
58. Mörner, A., I. Douagi, M. N. Forsell, C. Sundling, P. Dosenovic, S. O'Dell, B. Dey, P. D. Kwong, G. Voss, R. Thorstensson, et al. 2009. Human immunodeficiency virus type 1 Env trimer immunization of macaques and impact of priming with viral vector or stabilized core protein. *J. Virol.* 83: 540–551.
59. Haynes, B. F., P. B. Gilbert, M. J. McElrath, S. Zolla-Pazner, G. D. Tomaras, S. M. Alam, D. T. Evans, D. C. Montefiori, C. Karnasuta, R. Sutthent, et al. 2012. Immune-correlates analysis of an HIV-1 vaccine efficacy trial. *N. Engl. J. Med.* 366: 1275–1286.
60. Gottardo, R., R. T. Bailer, B. T. Korber, S. Gnanakaran, J. Phillips, X. Shen, G. D. Tomaras, E. Turk, G. Imholte, L. Eckler, et al. 2013. Plasma IgG to linear epitopes in the V2 and V3 regions of HIV-1 gp120 correlate with a reduced risk of infection in the RV144 vaccine efficacy trial. *PLoS ONE* 8: e75665.
61. Gorny, M. K., X. H. Wang, C. Williams, B. Volsky, K. Revesz, B. Witover, S. Burda, M. Urbanski, P. Nyambi, C. Krachmarov, et al. 2009. Preferential use of the VH5-51 gene segment by the human immune response to code for antibodies against the V3 domain of HIV-1. *Mol. Immunol.* 46: 917–926.
62. Gorny, M. K., J. Sampson, H. Li, X. Jiang, M. Totrov, X. H. Wang, C. Williams, T. O'Neal, B. Volsky, L. Li, et al. 2011. Human anti-V3 HIV-1 monoclonal antibodies encoded by the VH5-51/VL lambda genes define a conserved antigenic structure. *PLoS ONE* 6: e27780.
63. Stanfield, R. L., M. K. Gorny, C. Williams, S. Zolla-Pazner, and I. A. Wilson. 2004. Structural rationale for the broad neutralization of HIV-1 by human monoclonal antibody 447-52D. *Structure* 12: 193–204.
64. Pan, R., J. M. Sampson, Y. Chen, M. Vaine, S. Wang, S. Lu, and X. P. Kong. 2013. Rabbit anti-HIV-1 monoclonal antibodies raised by immunization can mimic the antigen-binding modes of antibodies derived from HIV-1-infected humans. *J. Virol.* 87: 10221–10231.
65. Pettersen, E. F., T. D. Goddard, C. C. Huang, G. S. Couch, D. M. Greenblatt, E. C. Meng, and T. E. Ferrin. 2004. UCSF chimera—a visualization system for exploratory research and analysis. *J. Comput. Chem.* 25: 1605–1612.